Minority Carrier Dynamics and Interfacial Kinetics at the ZnO/Electrolyte Interface Studied by Combined Photocurrent/Microwave Photoconductivity Measurements

Antonio M. Chaparro[†] **and Helmut Tributsch***

Hahn-Meitner Institut. Dept. Solare Energetik, Glienicker Strasse 100, 14109 Berlin, Germany

Received: January 7, 1997; In Final Form: May 21, 1997[⊗]

A pronounced peak of microwave photoconductivity (PMC), observed in the region of onset of photocurrents through a ZnO (0001)/aqueous electrolyte interface, is studied in dependence of electrolyte composition, electrochemical pretreatments, and light intensity. The amplitude, position, and shape of the peak were found to depend on interfacial kinetics, and the peak converts into a plateau with limiting PMC in the presence of an organic electrolyte. The PMC peak can be understood as an accumulation of minority carriers, the surface lifetime of which has increased due to limiting interfacial reactivity in charge transfer or recombination. The theory allows the determination of interfacial rate constants from parallel potentiodynamic PMC and photocurrent measurements. An exponential dependence of the charge transfer rate constant (k_r) on the applied voltage was found for ZnO in contact with different aqueous electrolytes at low electrode bias. This is in contradiction with classical models on photoelectrochemical charge-transfer which assume potential independent rate constants (Gärtner model as applied to electrodes: $k_r \rightarrow \infty$; Marcus−Gerischer model, k_r = const). The conclusion is that these models cannot be applied and that the condition of weak interaction during electron transfer is not fulfilled. The latter condition can however be approached with an organic electrolyte containing ferrocene/ferrocenium$^+$.

Introduction

The semiconductor/electrolyte (SC/EL) system has relevance in solar energy conversion, pollutants degradation, and semiconductor processing.[1] Its efficiency is limited in many cases by the rate of charge transfer at the SC/EL interface, which is the central process in any application. Up to now this process is poorly understood, most probably due to the lack of direct experimental access. The theories describing it[2,3] must rely on concepts from related fields (homogeneous and metal/electrolyte kinetics and solid-state physics) and with little support, if any, from direct experiments in an electrochemical cell (EC). One of the problems is that the rate of response of the EC is dominated by the time constant of the circuit, $R_{SOL}C_{SC} \approx 10^{-5}$s ($R_{SOL}$ is the solution resistance, and C_{SC} is the capacitance of the semiconductor space charge layer), or limited to the partial charging of the interfacial capacity, making the study of fast processes from (photo)current responses impossible. Experimental measurements on charge-transfer processes inside ECs have been obtained by indirect methods (e.g., measurement of the luminescence decay after a laser pulse), but are only able to give a rough estimation of relevant constants.[4−6]

Recently it has been shown that photoinduced microwave conductivity (PMC) in conjunction with photocurrent measurements allows a new insight into the photoelectrochemical process.[7−9] In fact, the power of this technique resides in that it involves the simultaneous measurement of the concentration of an intermediate species (minority carriers at the surface) and of the velocity of the charge-transfer reaction (photocurrent).[7] The photoelectrochemical process is schematized in Figure 1. After photogeneration in the space charge layer (SCL) under depletion conditions, minority charge carriers migrate to the SC surface. Minority carriers at the surface are involved in two competing reactions: (1) the photoelectrochemical reaction (i.e. transfer to redox levels in the electrolyte) and (2) recombination with electrons of the conduction band (Figure 1). In this scheme, the concentration of holes at the surface in the stationary state (ss) may be expected to depend on the velocities of the three processes involved:

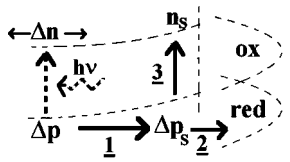

Figure 1. Kinetic scheme used in the theoretical analysis of PMC signals showing photogeneration and migration of holes in the space-charge layer of an n-type semiconductor (1), transfer to electrolyte reduced species (2), and surface recombination (3).

$$dp_s/dt = I_s - qk_r\Delta p_s - qs_r\,\Delta p_s = 0 \quad \text{(ss)} \tag{1}$$

$$\Delta p_s = I_s/q(k_r + s_r) \tag{2}$$

where Δp_s is the concentration of holes at the surface, k_r and s_r are the first-order rate constants for charge transfer and surface recombination, respectively, I_s is the photoinduced hole flux to the surface, and q is the elementary charge.

Measurement of Δp_s is carried out by the PMC technique.[7−8] Assuming a linear optical response of the semiconductor, a photoinduced change in the microwave absorption (microwave photoabsorption) arises from a photoinduced change in the imaginary part of the complex propagation constant ($\mathrm{Im}(\gamma^2) = \omega\mu(\sigma + \omega\epsilon'')$, where ω is the angular frequency of the radiation, μ is the permeability of the medium, σ is the electrical conductivity and ϵ'' is the imaginary part of the complex permittivity). For radiation energies just above the band gap ($h\omega/2\pi > E_g$), this change can be mainly attributed to the variation of the conductivity of the sample ($\Delta\sigma$), due to the increment in the free charge concentration. A contribution to $\Delta\sigma$ from dipoles may also take place if there is a photoinduced variation of the charge trapped at the surface or in the bulk,

* Corresponding author.
[†] On leave from Instituto de Catálisis y Petroleoquímica (CSIC), Camino de Valdelatas s/n, Cantoblanco 28049, Madrid, Spain
[⊗] Abstract published in *Advance ACS Abstracts,* August 15, 1997.

S1089-5647(97)00113-2 CCC: $14.00

although no experimental evidence of this contribution has been observed in microwave photoabsorption experiments apparently because it is much less significant.

Thus, to a good approximation, both photogenerated free electrons (Δn) and holes (Δp) give rise to microwave photoabsorption:

$$\mathrm{PMC} \sim \Delta\sigma = \Delta \mathrm{n}\mu_\mathrm{n} + \Delta p\mu_\mathrm{p} \quad (3)$$

where μ_n and μ_p are the mobilities for electrons and holes, respectively. For ZnO, it is $\mu_\mathrm{n} \approx \mu_\mathrm{p}$, so both type of free charge carriers contribute to the microwave photoabsorption. The signal measured in a PMC experiment corresponds to the stationary-state microwave photoabsorption (i.e., it is related to the stationary concentrations of carriers). Since electrical neutrality must be maintained inside the semiconductor ($\Delta n = \Delta \mathrm{p}$ in the absence of trapping), a stationary-state PMC signal requires the presence of excess carriers accumulated at the surface counterbalanced by excess carriers of opposite sign in the bulk. Therefore, the main requisite for the observation of a PMC signal is a long enough lifetime for carriers at the surface of the electrode, where lifetimes are usually much shorter. In this sense, the PMC technique is a surface sensitive technique. Experimental evidence for this will be given below.

An analytical expression for the stationary-state PMC signal under depletion conditions, containing physical parameters of the semiconductor and the interfacial kinetical constants has been calculated:[7]

$$\mathrm{PMC} = \mathrm{S}\{I_0(1 - \mathrm{e}^{-\alpha W}/(1 + L_\mathrm{p}\alpha))/(k_\mathrm{r} + s_\mathrm{r} + D\mathrm{e}^{-\Delta U q/kT}/L_\mathrm{p})\, 2^{1/2} L_\mathrm{D}\, \Phi(\Delta U)\} \quad (4)$$

where S is a calibration constant, I_0 is the light intensity entering the semiconductor, L_p and D are the diffusion length and diffusion coefficient of minority carriers, respectively, α is the absorption coefficient, L_D is the Debye length, ΔU is the band bending, W is the width of the space charge layer, k and T are the Boltzmann constant and absolute temperature, respectively, and $\Phi(\Delta U)$ is a function of the band bending, given by

$$\Phi(\Delta U) = \exp[-(\Delta U q/kT)^2] \int_0^{\sqrt{\Delta U\, q/k\, T}} \exp(t^2)\mathrm{d}t \quad (5)$$

$\Phi(\Delta U)$ accounts for the change in microwave absorption due to redistribution of minority carriers upon changing the band bending. The analytic expression in eq 4 has been calculated for a silicon Schottky barrier and was found to coincide within 10% with the unsimplified numeric function.[8] It is valid for L_p, $1/\alpha > L_\mathrm{D}$, and $\Delta U > kT/q$. In the case of ZnO the corresponding values are $L_\mathrm{p} = 15$ μm (determined from microwave transients), $1/\alpha = 0.05$ μm (for $\lambda = 330$ nm) and $L_\mathrm{D} = 0.03$ μm (for $N_\mathrm{D} = 10^{16}$ cm^{-3}), so eq 4 is sufficiently justified.

The plot of PMC vs ΔU for depletion conditions of a ZnO electrode is shown in Figure 2A for two limiting values of k_r. For slow charge transfer ($k_\mathrm{r} \rightarrow 0$), a sharp increase is observed at low band bending due to minority carriers accumulation at the surface. Upon increasing the band bending, the PMC signal attains a maximum and then diminishes slowly because the faster drift of carriers leads to a change in their concentration profile. On the other hand, for very high charge transfer rate ($k_\mathrm{r} \rightarrow \infty$), no accumulation of minority carriers takes place at the surface and no PMC signal is consequently observed under depletion conditions. The photocurrent responses (I_ph) calculated for the same model are shown in Figure 2B. The photocurrent

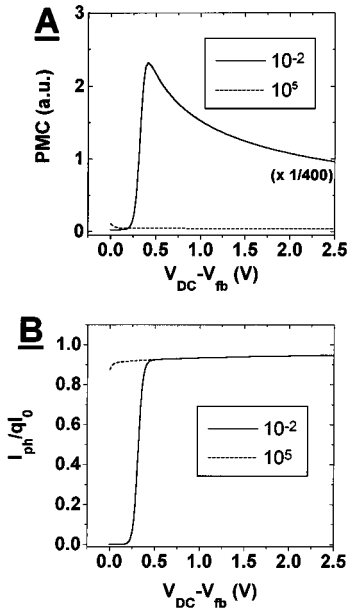

Figure 2. Calculated PMC (A) and photocurrent (B) signals from eq 4 and eq A25 of ref 7, respectively. The values for the parameters are $S = 1$ cm^{-2}, $I_0 = 1$ cm^2 s^{-1}, $s_\mathrm{r} = 0.01 \exp(-q\ \Delta U/kT)$, $\alpha = 6000$ cm^{-1}, $D = 4.62$ cm^2 s^{-1}, $L_\mathrm{D} = 0.03 \times 10^{-4}$ cm, $L_\mathrm{p} = 15 \times 10^{-4}$cm. k_r values are 0.01 cm s^{-1} and 10^5cm s^{-1} for solid curve and dash curve, respectively.

corresponding to the velocity of process 2 (Figure 1) is given by

$$I_\mathrm{ph} = qk_\mathrm{r}\, \Delta p_\mathrm{s} \quad (6)$$

On the other hand, the recombination current, characterizing process 3 in Figure 1, is obtained according to

$$I_\mathrm{s} - I_\mathrm{ph} = qs_\mathrm{r}\, \Delta p_\mathrm{s} \quad (7)$$

where I_s is the flux of minority carriers to the interface, which can be calculated. For instance, a simple expression was deduced by Gärtner[10] which does not consider bulk recombination kinetics:

$$I_\mathrm{s}\, I_0[1 - \mathrm{e}^{-\alpha W}/(1 + \alpha L_\mathrm{p})] \quad (8)$$

More elaborated theories include it.[11,12] Equation 8 equals the photocurrent when the velocity of interfacial charge transfer is much higher than the velocity of recombination ($k_\mathrm{r} \gg s_\mathrm{r}$). Equations 4−8 rationalize combined PMC and photocurrent measurements. They include three unknowns related by eq 2 (Δp_s, k_r, and s_r), which describes the interfacial kinetics of the system in the stationary state. These parameters, as well as their evolution with the applied potential in the photoelectrochemical cell, can be obtained from combined PMC−photocurrent measurements, provided the other physical parameters of the semiconductor and the calibration constant for PMC (S) are known. (This constant can be obtained from a measurement of PMC under flat-band conditions if $\Delta p_\mathrm{s} \approx 0$).[7b]

Early PMC measurements with ZnO indicated the presence of a pronounced peak in the region of onset of anodic photocurrent.[13] The aim of our study was to investigate this phenomenon and to study its dependence on electrochemical parameters in the light of a better theoretical background on microwave−electrochemical phenomena.[7,8] The main focus of our work will be on getting more detailed information on interfacial rate constants for electronic charge transfer involving the valence band of this large gap ($E_\mathrm{g} = 3.2$ eV) semiconductor.

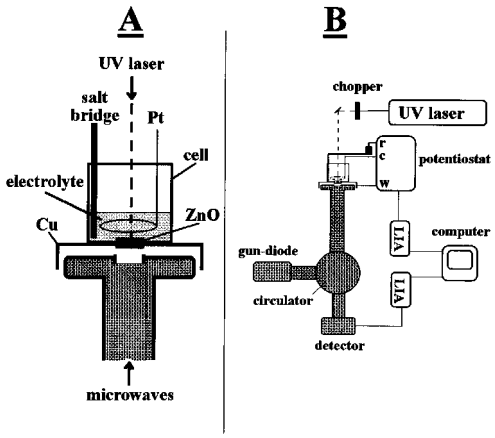

Figure 3. Photoelectrochemical cell (A) and experimental setup (B) for simultaneous PMC and photocurrent measurements.

The theory of microwave−electrochemistry as applied to ZnO allows the determination of the interfacial rate constant via the relation:[8]

$$k_r(\Delta U) \propto I_{ph}\Phi(\Delta U)/\mathrm{PMC} \qquad (9)$$

For the simple Gärtner model applied to an illuminated semiconductor electrode under depletion conditions, k_r must go to infinity and the positive PMC peak disappears (Figure 2). On the other hand, the classical Marcus model (weak interaction), as applied by Gerischer, predicts a constant rate for isoenergetic charge transfer (since a shift of energy bands can be neglected within certain potential limits) according to the relation[2]

$$k_r = k_{r0}\exp\{-(E_{VB} - E_{RED})^2/4\lambda kT\} \qquad (10)$$

where k_{r0} is a constant including the thermal velocity of holes in the valence band and the concentration of reduced species or hole acceptors at the surface, λ is the reorganization energy, E_{VB} is the energy of the upper valence band edge at the surface, and E_{RED} is the mean energy of the electronic level of the reduced species involved in the reaction. In this case, a positive PMC peak is expected, as indicated in Figure 2. This signal increases very fast with increasing positive potential and beyond the peak decreases slowly (50% with a potential change of 2 V). Any deviation from the constant rate predicted by the Marcus−Gerischer model can be calculated from potential dependent PMC and photocurrent data according to eq 9.

Experimental Section

ZnO single crystals ($\sigma = 1.41 \times 10^{-3}\ \Omega^{-1}\mathrm{cm}^{-1}$) of about 1 mm thickness were mounted in specially designed electrochemical cells (Figure 3A), exposing to the electrolyte an area of ca.1 mm^2 corresponding to (0001) or (000$\bar{1}$) faces. The back contacts were made with silver paste (Ecolit), and isolated with epoxy resin (Scothcast, 3 M). The applied potential in the electrochemical cell was controlled with a potentiostat (Wenking, Pos 73). A platinum wire was used as counter electrode and a mercury sulfate electrode (MSE) as reference. Aqueous electrolytes were made with reagent grade chemicals and triply destilled water. For the experiments in nonaqueous electrolyte, a solution of propylene carbonate (PC) containing 0.6% water (Merck) dried over molecular sieves (4 Å pore diameter), with 0.1 M tetrabutylammonium perchlorate (TBAP) as conducting salt, and ferrocene/ferrocenium$^+$ (Cp_2Fe/Cp_2Fe^+) as redox couple, was used. In this case, the applied potential was measured against Cp_2Fe/Cp_2Fe^+ ($E^0 = -0.1$ V/MSE) by means of a platinum wire. Flat-band potentials (V_{fb}) within ±100 mV were taken from the potential at which the PMC signal starts in a voltammogram from accumulation to depletion.[7]

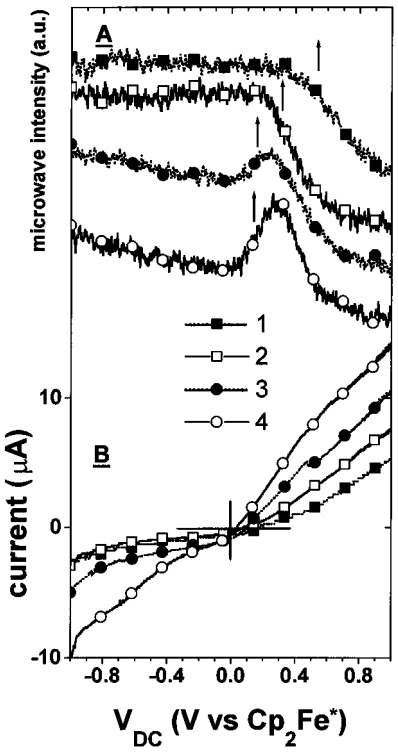

Figure 4. PMC (A) and total current (B) measured on ZnO single crystal in contact with PC, 0.1 M TBAP, 10^{-2} M Cp_2Fe solution (curves 1). Curves 2, 3, and 4 correspond to the addition of 5%, 10%, and 20% volume of water, respectively. Illumination with He:Cd UV laser (5mW), modulation frequency 70 Hz, $v = 2$ mV s^{-1}. The arrows indicate the onset potential for the photocurrent (V_{on}).

The experimental setup for combined PMC−photocurrent measurements has already been described[9] and is depicted for completeness in Figure 3B. The UV light source (Laser He-Cd, Omnichrome model 1001.2 mm beam diameter) is mechanically chopped (HMS, Light Beam Choper 220) and directed toward the surface of the photoelectrode in contact with the electrolyte. Microwaves are generated by a Gunn-diode and directed toward the photoelectrode back surface, which is not in contact with the electrolyte. The microwave power reflected from the electrolyte contact is measured with a microwave detector and amplified with lock-in (SR510). At the same time the photocurrent passing through the electrochemical cell is measured with a second lock-in (EG&G PARC 5205). Data are collected and stored with a McIntosh computer.

Results

Measurements with organic solvent. PMC voltammograms corresponding to monocrystalline ZnO in propylene carbonate (PC), 0.1 M TBAP, 10^{-2} M Cp_2Fe solution, and after addition of different amounts of water, are shown in Figure 4. When no water is present in the electrolyte, a constant PMC signal in the negative range of potentials is observed that starts to diminish at $V_{DC} = 0.3$ V, just before the onset of photocurrent (V_{on}) is observed (V_{on} values are indicated by an arrow in Figure 4), and then, at $V_{DC} = 0.9$ V attains a second lower plateau (Figure 4A, curve 1). Upon addition of water the shape of the PMC signal and the total current flowing through the cell change significantly. A progressive diminution of the PMC signal is observed in the negative range of potentials, giving rise to a peak shape signal located 200 mV positive from V_{on} (Figure

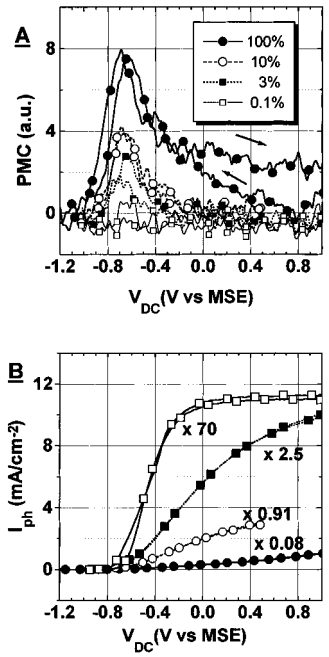

Figure 5. Simultaneously recorded PMC (A) and modulated photocurrent voltammograms (B) corresponding to ZnO in contact with 1 M KCl at different illumination intensities (100% correspond to 12.5 mW output laser power). The photocurrent curves have been multiplied by $1/I_0$ to facilitate comparison of the shapes. Illumination with UV laser (He:Cd), modulation frequency $f = 60$ Hz, $\upsilon = 10$ mV s^{-1}.

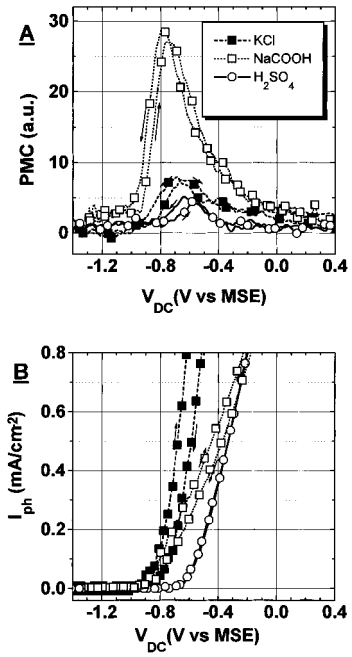

Figure 6. PMC (A) and modulated (lock-in) photocurrent voltammograms (B) corresponding to ZnO in contact with three different electrolytes: 1 M KCl, 1 M NaCOOH and 0.5 M H_2SO_4. He:Cd laser (12.5 mW), $f = 60$ Hz, $\upsilon = 10$ mV s^{-1}.

4A, curves 2−4). At the same time, an increment in the total current is observed upon addition of water (Figure 4B). It must be pointed out that the reference voltage is probably changing from one voltammogram to the other due to the change of the composition of the electrolyte (notice the shift in V_{on}), but this is not important for the purpose of this experiment.

Measurements in Aqueous Solution. In 100% aqueous solutions, only a peak is observed in the PMC voltammogram, as shown in Figure 5A, for various illumination intensities. The peak is located at $V_{DC} = -0.65$ V/MSE, slightly positive from the photocurrent onset ($V_{DC} = -0.85$ V/MSE), although it must be noticed that the peak starts approximately at the same potential as the photocurrent (V_{on}). The photocurrent curves (Figure 5B) have been normalized by multiplying by $1/I_0$ in order to compare the shapes of the curves. A clear diminution in the slope of the rising part with increasing light intensity is observed. Only at lower intensities (3% and 0.1%) a plateau is attained indicating hole flux limitation in the photoelectrochemical reaction.

Figures 6 and 7 show PMC (A) and photocurrent (B) voltammograms simultaneously obtained with ZnO in contact with three different electrolytes, 1 M KCl, 1 M NaCOOH, and 0.5 M H_2SO_4, and two light intensities. A change both in the height and in the position of the PMC signal is observed upon variation of the electrolyte composition. The highest PMC intensity is observed with 1 M NaCOOH electrolyte, where it is placed at −0.80 V/MSE for negative sweep and −0.75 V/MSE for positive sweep. With KCl, the PMC peak has lower intensity and is placed at more positive potential (−0.70 V negative sweep and −0.63 V/MSE positive sweep). Notice, however, that the slope of the photocurrent curve is higher with KCl electrolyte than with NaCOOH. For H_2SO_4, the peak is at more positive potentials, −0.65 V/MSE for negative and −0.57 V/MSE for positive scan, as well as the onset for photocurrent (−0.75 V/MSE). Less intense PMC peaks without significative changes in the shapes and positions are observed with lower light intensity (1.1 mW output laser power) (Figure 7). In this case, the slope of the photocurrent curve for HCOONa is higher than at high illumination intensity (Figure 6) at the same time that the PMC peak shows now the same intensity as for KCl solution. Both effects are related to changes in the reactivity of holes at the surface as a consequence of illumination intensity.

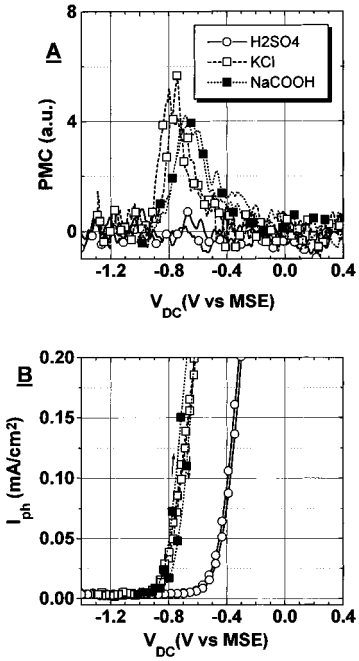

Figure 7. PMC (A) and modulated photocurrent voltammograms (B), as in Figure 5, with 1.1 mW illumination.

Discussion

In organic solvent, the electrochemistry of ZnO is much simpler than in aqueous solution. Reactions such us the formation of metallic Zn at negative potentials or the dissolution of the lattice at positive potentials are hindered because of the absence of water. Under such conditions of low surface

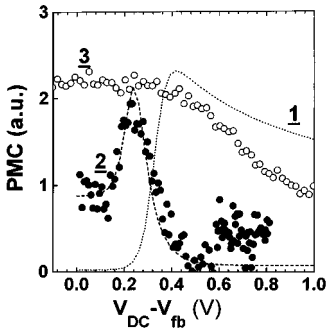

Figure 8. Calculated PMC signals (eq 4) taking $k_r = 0.01$ cm s^{-1} (1) and $k_r = 0.01\exp(-0.4\Delta Uq/kT)$ (2) (other parameters as in Figure 2). Also shown are the experimental PMC curves for ZnO/0.5M H_2SO_4 (solid circle) and for ZnO/PC, 0.1 M TBAP, 10^{-2} M Cp_2Fe (open circles, 3).

reactivity, efficient polarization of the space charge layer by application of negative potentials (vs V_{fb}) is possible giving rise to accumulation of conduction band electrons at the interface, to the formation of high electric field in the space charge layer, and to the repulsion of positive carriers from the electrode interface toward the interior. This phenomenon is responsible for the negative plateau reached for the PMC signal in the complete absence of water (Figure 4, curve 1). Addition of water to the solution introduces a reactant for free carriers at the semiconductor−electrolyte interface that reduces their surface lifetime. That produces a diminution of the PMC plateau due to electrons at the interface because they are now less efficiently accumulated, and an increment of the reduction current (Figure 4, curves 2−4). With higher amounts of water the reactivity of electrons increases, yielding the disappearance of their PMC signal and leaving a peak in a range of potential close to the photocurrent onset. Such a signal corresponds to the accumulation of photogenerated holes migrating to the interface. In aqueous electrolyte (Figures 5A−7A) this peak shows constant position with respect to photocurrent onset, irrespective of the composition of the electrolyte and/or the surface pretreatment, indicating that free holes are always accumulated at the interface at low band bending. (Also trapped holes in surface sites leading to a change in dipole conductivity could in principle be responsible for this peak, but it is less probable that they could produce an observable change in microwave photoabsorption). On the other hand, the intensity and width of the PMC peak are sensitive to the electrolyte composition (Figure 6) due to differences in surface reactivity of holes, as shown below.

The experiments with different light intensities show a correlation between the slope of the photocurrent curve and the height of the PMC peak (Figure 4). Total photon to current conversion is only attained at the lowest intensity, when the photocurrent voltammogram shows a plateau and no PMC signal is observed. Upon increasing the light intensity, no saturation value is observed for the photocurrent and, at the same time, the PMC signal rises. That reflects that an important accumulation of holes at the surface takes place because the transfer velocity is not high enough. Limiting interfacial transfer velocity is therefore responsible for the decrease in the quantum efficiency.

A slow interfacial transfer rate which produces accumulation of minorities indicates that the Gärtner model ($k_r \rightarrow \infty$) is not applicable to electrochemical interfaces. The Gerischer−Marcus model, on the other hand, which assumes a potential independent rate constant (eq 10) predicts a PMC-signal with a slow decay upon increasing the applied electrical potential (Figure 2). In Figure 8 the experimental PMC peak obtained for aqueous H_2SO_4 electrolyte is plotted together with a calculated PMC signal using eq 4. In order to obtain a good fit, an exponentially increasing rate constant of the form

$$k_r = k_{r0}\exp\{\gamma q\Delta U/kT\} \qquad (11)$$

with $\gamma = 0.4$ has been used (also is shown the curve for $k_r =$ const for comparison). A reasonable coincidence between theory and experimental data is observed. The departure of the behavior of the ZnO/H_2SO_4 system from that predicted by Marcus−Gerischer model (curve 1) is evident. Also shown in Figure 8 is the PMC signal corresponding to the organic solvent (curve 3). Although the signal due to accumulation of electrons is superimposed to that of holes in curve 3, however, the decaying part at positive potentials from V_{on} can be solely attributed to holes at the surface. It must be noticed that this decay is clearly less pronounced than for aqueous electrolytes and reflects a behavior closer to the Marcus−Gerischer model (curve 1).

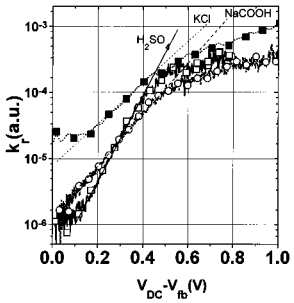

Figure 9. Dependence of the charge transfer constants (k_r) on the band bending (ΔU) obtained by application of eq 9 to combined PMC−photocurrent measurements corresponding to ZnO in contact with 1 M NaCOOH, 1 M KCl, and 0.5 M H_2SO_4.

TABLE 1

electrolyte	V_D (V/MSE)	I_0 (mW)	PMC_{peak} (au)	I_{ph} (μA)
0.5 M H_2SO_4	−0.60	12.5	5	0.50
0.5 M H_2SO_4	−0.60	1.1	0.5	0.05
1 M KCl	−0.65	12.5	8	4.00
1 M KCl	−0.65	1.1	4	2.00
1 M NaCOOH	−0.78	12.5	29	0.75
1 M NaCOOH	−0.78	1.1	5	0.40

Full analysis of the dependence of k_r on ΔU can be made by application of eq 9 to the experimental PMC and photocurrent measurements. This is carried out in Figure 9 for the three electrolytes 0.5 M H_2SO_4, 1 M KCl, and 1 M HCOONa, showing the exponential dependence of k_r on ΔU as given by eq 11. From the slope of the right portions it is possible to determine experimental "transfer coefficients" (γ, eq 11) of 0.40, 0.24, and 0.20 for H_2SO_4, NaCOOH, and KCl, respectively. The electrochemical reactions which must be considered, besides photodissolution and parallel corrosion, are oxygen evolution from water (in case of H_2SO_4) and oxidation of Cl^- anions and of $HCOO^-$ in the low potential region.[14−16] In the case of $HCOO^-$, photodissolution also seems to take place as part of a current doubling mechanism.[17] It must be said, however, that PMC experiments do not yield information on the detail mechanisms of the reactions involved, but on the dynamics of carriers at the surface.

It appeared to be interesting to perform a comparative study of the reactivity in aqueous solution. The differences in the combined PMC−photocurrent results shown in Figure 6 and 7 for the three electrolytes KCl, HCOONa, and H_2SO_4 reflect different reactivities of holes at the surface. In Table 1 the values for the intensity of the PMC peak and of the photocurrent passing at the peak voltage are shown for the three electrolytes

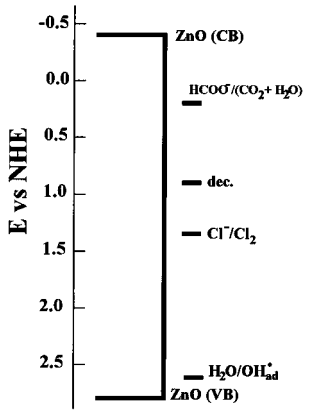

Figure 10. Energy scheme showing the bands of ZnO and the redox energy of the reactions in aqueous solution; dec. corresponds to the photodecomposition of ZnO in the presence of Cl^- (pH = 7) according to ref 19.

studied and two different illumination intensities. It is remarkable that a high intensity of the peak for NaCOOH is observed simultaneously with a photocurrent value which is 1 order of magnitude lower than in the case of KCl. For this latter system, the peak is, on the other hand, less pronounced. Supposing that the band bending at the PMC peak is the same, reasonable within ±100 mV,[7] then the following relation arises from eq 9:

$$(k_r)_i/(k_r)_j = [\mathrm{PMC}_j I_{ph,i}]/[\mathrm{PMC}_i I_{ph,j}] \quad (12)$$

$$(s_r)_i/(s_r)_j = [\mathrm{PMC}_j(I_s - I_{ph,i})]/[\mathrm{PMC}_i(I_s - I_{ph,j})] \quad (13)$$

where the subindexes *i*, *j* are for different electrolytes. By applying the expressions to the values in Table 1 at the potential of the PMC peak, one obtains the following series for the rate constants at two output laser powers (*I*):

$$(k_r)_{Cl} = 5\,(k_r)_{dec} = 20\,(k_r)_{HCOO} \qquad I = 12.5\ \mathrm{mW}$$

$$(s_r)_{dec} = 1.6\,(s_r)_{Cl} = 6\,(s_r)_{HCOO} \qquad I = 12.5\ \mathrm{mW}$$

$$(k_r)_{Cl} = 5\,(k_r)_{dec} = 6\,(k_r)_{HCOO} \qquad I = 1.1\ \mathrm{mW}$$

$$(s_r)_{dec} = 8\,(s_r)_{Cl} = 10\,(s_r)_{HCOO} \qquad I = 1.1\ \mathrm{mW}$$

These sequences reflect that hole transfer is faster to Cl^- ions at high and low illumination intensities, in comparison with the other two electrolytes. On the other hand, the transfer of holes to $HCOO^-$ anions is the most difficult, mainly at high illumination intensity. That means that a high concentration of holes at the surface diminishes the efficiency of the transfer mechanisms (see also the change in the slope of the voltammograms upon variation of the light intensity in Figures 6 and 7). Recombination processes are also slower in NaCOOH, but they become comparatively faster at high illumination intensity, as opposed to charge transfer. In H_2SO_4 solution, where photodisolution of ZnO takes place surface recombination is faster at high and low intensities and competes more efficiently with the faradaic process. The redox energies of the reactions can be compared with the position of the bands of ZnO in a kind of scheme frequently used in kinetics studies (Figure 10). The relative position of the energy levels and the k_r sequences in eqs 14 and 16 are in accordance with the Marcus−Gerischer model, although opposite results have also been obtained from current-doubling measurements.[15] In fact, schemes as in Figure 10 are of poor value in reactions governed by strong interactions or mediated by surface states.

As explained in the introduction, parallel potential dependent measurements of photocurrent and PMC permit the determination of interfacial rate constants. The formulas taken into consideration (eqs 4−8), consider only reactions of semifree minority carriers (in the space charge layer) but do not describe any reaction of this carriers after being trapped or transfered to surface states. The interfacial reaction rates determined therefore describe global reaction rates for the passage of charge carriers to the electrolyte and do not permit expecifications of partial reaction steps. The acceptor distribution of surface mediated pathways can for example not be evaluated. The most remarkable result for the ZnO/aqueous electrolyte interface is that the interfacial rate constant depends exponentially on the applied electrode potential for this quite ideal semiconductor (single crystal, slowly dissolving oxide, and large energy gap). This fact cannot be explained in the light of the classical Gerischer model, if we reasonably assume that no significant change in the Helmholtz potential is taking place in the range of potentials studied. In fact, this assumption is supported by the good linearity always encountered in Mott−Schottky plots of ZnO.[18] The situation suggests the necessity to consider other models for the charge transfer at the SC/EL interface able to explain the influence of electric fields of the space charge layer and Helmholtz layer. Experimental evidence on electrical field induced charge transfer have been reported by Rosenwaks et al.[6] based on transient photoluminescence experiments on a p−InP semiconductor. In this case, mathematical solution of the Poissons equation was necessary to discriminate the effect of the electric field on charge transfer from that on separation and surface recombination of charge carriers. They discussed the participation of hot carriers in the charge transfer process as possibly contributing to the effect. Such a mechanism cannot be excluded for ZnO and requires further analysis (also thermally relaxed holes may become accelerated by the electric field in the semiconductor surface). Another possibility would be to consider an influence of the electric field on the interactions between the semiconductor surface and electroactive species, a factor not included in the Gerischer model. In fact, the results of Figure 8 point in this direction, where the faster decay of the PMC signal in aqueous solution (curve 2) reflects that the interaction of water molecules with the surface of the electrode is real responsible for the peak shape PMC signal, (i.e., for the faster hole transfer). Notice, however, that in curve 3 (100% organic solvent) the decay of the signal still differs from that corresponding to electric field independent rate constant (curve 1). Mediation of surface states in charge transfer reaction can also give rise to a potential dependent rate constant if the position and filling of the levels changes with the applied potential (and the corresponding change in the Helmholtz layer).

Conclusions

Combined microwave−photocurrent measurements have been used to make a comparative study of the reactivity of holes at a ZnO/electrolyte interface. By application of a kinetic model to the experimental results, an exponential dependence of the charge transfer constant on the applied voltage is revealed in contact with aqueous electrolytes, which cannot be explained by classical theories. It may be concluded that the charge transfer reactions observed in aqueous electrolytes are controlled by potential dependent extrinsic surface states (interaction with water) or are dominated by strong interactions. Comparison with experiments in noninteracting organic solvents indicate that interactions between solvent and surface of the electrode play indeed an important role in the electrochemical reaction. Also attention should be paid to the possibility that reacting charge

carriers (forward or backward reaction) may not be in thermal equilibrium but their kinetical energy affected by the electrical field in the surface near the space charge layer. In this way the electron transfer would become increasingly irreversible with increasing potential and photocurrent flow. More experimental evidence and theoretical analysis are necessary to explain the described effect.

Acknowledgment. Thanks are due to F. Wünsch for his help with the experimental setup. In addition, we thank Prof. Salvador and Dr.Schlichthörl for stimulating discussions and Dr. Pohlmann for critically reading the manuscript. A. M. C. acknowledges a postdoctoral grant from Ministerio de Educación y Cultura (Spain).

References and Notes

(1) Tributsch, H. In *Photocatalysis and Environment: Trends and Applications*; Schiavello, M., Ed.; 297−347; Kluwer Academic Publishers: Dordrecht, **1988**; Vol. C237 p 297−347.

(2) Gerischer, H. In *Advances in Electrochemistry and Electrochemical Engineering*; Delahay, P., Tobias, W., Eds.; Interscience: New York, 1961; Vol. 1 p 139.

(3) Marcus, R. A. *J. Chem. Phys.* **1965**, *43*, 679−701.

(4) Lewis, N. S. *Annu. Rev. Phys. Chem.* **1991**, *42*, 543−580.

(5) Evenor, M; Gottesfeld, S.; Harzion, Z.; Huppert, D.; Feldberg, S. W. *J. Phys. Chem.* **1984**, *88*, 6213−6218.

(6) Rosenwaks, Y.; Thacker, B. R.; Nozik, A. J.; Ellingson, R. J.; Burr, K. C.; Tang, L. C. *J. Phys. Chem.* **1994**, *98*, 2739−2741.

(7) (a) Schlichthörl, G.; Tributsch, H. *Electrochim. Acta.* **1992**, 37, 919−931. (b) Schlichthörl, G. Ph.D. Thesis, Freie Universitat, Berlin, 1992.

(8) Tributsch, H.; Schlichthörl, G.; Elstner, L. *Electrochim. Acta.* **1993**, *38*, 141−152.

(9) Wünsch, F.; Nakato, Y.; Kunst, M.; Tributsch, H. *J. Chem. Soc., Faraday Trans.* **1996**, *92*, 4053−4059.

(10) Gärtner, W. W. *Phys. Rev.* **1959**, *116*, 84

(11) Reiss, H. J. *J. Electrochem. Soc.* **1978**, *125*, 937

(12) Wilson, R. H. *J. Appl. Phys.* **1977**, *48*, 4292

(13) Bogomolni, R. A.; Tributsch, H.; Petermann, G.; Klein, H. *J. Chem. Phys.* **1983**, *78*, 2579−2584.

(14) Morrison, S. R.; Freund, T. *J. Chem. Phys.* **1967**, *47*, 1543−1551.

(15) Freund, T.; Gomes, W. P. *Catal. Rev.—Sci. Eng.* **1969**, *3*, 1−36.

(16) Gomes, W. P.; Freund, T.; Morrison, S. R. *J. Electrochem. Soc.* **1968**, *115*, 818−823.

(17) Schoenmakers, G. H.; Vanmaekelbergh, D.; Kelly, J. J. *J. Chem. Soc., Faraday Trans.* **1997**, *93*, 1127−1132.

(18) Lohmann, F. *Ber. Bunsen-Ges. Phys. Chem.* **1966**, *70*, 87−92.

(19) Gerischer, H. *J. Electroanal. Chem.* **1977**, *82*, 133−143.